

The photophysics of some 3-hydroxyflavone derivatives in the presence of protons, alkali metal and alkaline earth cations

Xavier Poteau^a, Ginagunta Saroja^a, Cathrin Spies^b, Robert G Brown^{a,c,*}

^a Centre for Photochemistry, University of Central Lancashire, Preston, Lancashire PR1 2HE, UK

^b Hamburger Synchrotronstrahlungslabor HASYLAB at Deutsches Elektronen-Synchrotron DESY, Notkestr. 85, D-22603 Hamburg, Germany

^c School of Applied Sciences, University of Glamorgan, Pontypridd CF37 1DL, UK

Received 13 June 2003; received in revised form 1 September 2003; accepted 10 September 2003

Abstract

The absorption and fluorescence properties of three monoaza crown ether (either 15-crown-5 or 18-crown-6 substituted at the 4'-position) 3-hydroxy- and 3-methoxy-flavone compounds in the presence of protons, alkali metal and alkaline earth cations are reported. The corresponding 4'-dimethylamino-flavones were also studied for comparison. All the compounds protonate in moderate acid (tens of mM H⁺) with significant changes in emission only being observed for the 3-methoxy derivatives. The crown ether compounds bind the alkaline earths with binding constants of the order of 10⁴ dm³ mol⁻¹ and with two moles of metal ion being bound at high concentrations.

© 2004 Elsevier B.V. All rights reserved.

1. Introduction

Among the various methods employed for sensing chemical species, fluorescent sensors offer distinct advantages in terms of sensitivity, selectivity and their ability to be applied as remote sensors. There is considerable current interest in the design, synthesis and characterisation of fluorescent sensors for both charged and neutral species particularly with biomedical and environmental applications in mind and the field has been extensively reviewed [1]. In particular, there has been continuing effort in the development of fluoroionophores which link a cation-selective ligand with a fluorescent probe for monitoring low concentrations of alkali and alkaline earth metal cations in solution, with real biological applications in mind [2].

Fluorescent sensors which exhibit two (or more) emission bands, whose relative intensity changes in the presence of an analyte, are particularly attractive. Létard et al. [3] have succinctly pointed out that the intensity ratio of the two bands can be related to analyte concentration and will be unaffected by variations in sensor concentration (e.g. due to photobleaching) or changes in the intensity of the excitation light. Rettig and Lapouyade [4] have reviewed the use of molecules which form TICT (twisted intramolecular charge

transfer) states as fluorescent probes and sensors—TICT molecules are one example of systems which can exhibit two or more emission bands [5]. Other possibilities include molecules which undergo excited state intramolecular proton transfer (ESIPT) [6] or excimer formation [7].

The 4'-dialkylamino derivatives of 3-hydroxy- and 3-methoxy-flavone (particularly 4'-*N,N*-dimethylamino-3-hydroxyflavone (**1a**) and 4'-*N,N*-diethylamino-3-hydroxy flavone (**2a**)) are believed to undergo both ESIPT and to form TICT states [8]. Our experience with these systems, which can be quite highly fluorescent, suggested that the replacement of the dialkylamino function with an aza crown ether could produce a ratiometric fluorescent sensor [9]; a conclusion reached completely independently by Roshal et al. [10,11]. Additionally, Wang and Wu have reported a related system with a 12-crown-4 ring attached at the 3-hydroxyl position [12]. Indeed, the sensitivity of the fluorescence spectra of these flavonols to their environment has suggested their potential use in a variety of applications, including sensing of hydrochloric acid [13], metronidazole [14] and the water content of acetone [15], as probes of protein-binding-sites [16], membranes [17] and micelles [18] and as potential laser dyes [19]. Klymchenko et al. have elaborated the structure of **2a** by replacing the dimethylaminophenyl moiety with a diethylamino-benzofuran group, producing a system with significantly red-shifted absorption and emission properties [20].

* Corresponding author. Tel.: +1-443-482280; fax: +1-443-48355.
E-mail address: rgbrown@glam.ac.uk (R.G. Brown).

The emission properties of **1a** and **2a** (in acetonitrile/benzene mixtures) were first reported by Swinney and Kelley [21] and by Chou and co-workers [19,22]. The spectra exhibit two emission bands whose position and intensity are strongly solvent and temperature dependent [8,21–24]. Both compounds are generally more fluorescent than the parent 3-hydroxyflavone, especially in polar solvents, and the ESIPT process which converts the excited “normal” species N^* to the proton-transferred tautomer P^* is closely intertwined with intramolecular charge transfer. In **2a** and **3a**, Nemkovitch et al. [25] suggest that charge and proton transfer alternate in the excited state, ie following excitation of N^* , the main excited state charge transfer event precedes ESIPT, but there is further excited state charge transfer following the proton transfer. We have proposed that TICT state formation competes with ESIPT [8], which may also explain the difference in properties between **1b** and a close analogue where the 3-oxygen is linked to the 2'-position of the phenyl ring with a methylene bridge [24].

In this paper we report the results of our investigations of the properties of several 4'-dialkylamino-3-hydroxyflavones in the presence of positively charged ions. The compounds investigated are 4'-*N,N*-dimethylamino-3-hydroxyflavone (**1a**) and its 3-methoxy derivative (**1b**) together with two analogues where the dimethylamino group is replaced by an aza crown ether; either a 15-crown-5 ether (**3a** and **3b**) or an 18-crown-6 ether (**4a**).

2. Experimental

Compounds **1a** and **1b** were prepared according to the published procedures [8]. Compounds **3a** and **4a** were prepared from *N*-phenyldiethanolamine via the *N*-phenylaza-15(18)-crown-5(6) (using the methods of Dix and Vögtle [26] and Schultz et al. [27]), their 4-formyl derivatives [26] and subsequent coupling of the latter with 2-hydroxy-acetophenone to yield **3a** (m.p. 133.8–134.5 °C) and **4a**.

3a ^1H NMR (250 MHz, CDCl_3): δ 3.57–3.77 (s + t, 20H, crown ether), 6.71(d, 2H, $\text{H}_{3',5'}$), 6.82 (s, 1H, OH), 7.32 (t, 1H, H_7), 7.50 (d, 1H, H_8), 7.59 (t, 1H, H_6), 8.10 (d, 2H, $\text{H}_{2',6'}$), 8.20 (d, 1H, H_5). Anal. Calcd for $\text{C}_{25}\text{H}_{29}\text{NO}_7$: C, 66.50; H, 6.49; N, 3.10%. Found: C, 66.71; H, 6.57; N, 2.79%.

4a ^1H NMR (250 MHz, CDCl_3): δ 3.66–3.72 (m, 24H crown ether), 6.74 (d, 2H, $\text{H}_{3',5'}$), 6.89 (s, 1H, OH), 7.42 (t, 1H, H_7), 7.65 (dd, 2H, $\text{H}_{5,6}$), 8.25 (dd, 1H, H_8).

Anal. Calcd for $\text{C}_{27}\text{H}_{33}\text{NO}_8$: C, 64.90; H, 6.60; N, 3.10%. Found: C, 64.73; H, 6.64; N 3.35%

3b was prepared by methylation [8] of **3a** and was recrystallised from ethyl acetate/hexane to yield a cream yellow powder (m.p. 156.9–157.3 °C).

^1H NMR (250 MHz, CDCl_3): δ 3.64–3.84 (s+t, 20H, crown ether), 3.89 (s, 3H, CH_3), 6.76 (d, 2H, $\text{H}_{3',5'}$), 7.26 (t, 1H, H_7), 7.37 (d, 1H, H_8), 7.51 (t, 1H, H_6), 8.10 (d, 2H, $\text{H}_{2',6'}$),

8.23 (d, 1H, H_5). Anal. Calcd for $\text{C}_{26}\text{H}_{32}\text{NO}_7$: C, 66.35; H, 6.87; N, 2.98%. Found: C, 66.21; H, 6.50; N, 2.89%.

All organic solvents were spectroscopic grade from Aldrich and were used as received. Water was doubly distilled and purified by ion exchange. Alkali metals and alkaline earths were all employed as their perchlorates (Analar grade) from either Fisher Ltd or Aldrich and were used as received.

Absorption spectra were recorded on a Hewlett-Packard HP8452A diode array spectrometer and fluorescence spectra on a SPEX Fluoromax. All spectra were corrected for the wavelength-dependent response of the spectrometer. The concentrations of the flavones used in the measurements were always in the range $1.0\text{--}2.0 \times 10^{-5} \text{ mol dm}^{-3}$. Fluorescence decay profiles were measured by the time-correlated, single photon counting technique [28] using synchrotron sources and instrumentation at the Daresbury Laboratory, Warrington [29] and HASYLAB, Hamburg [30]. The decay profiles were analyzed by computer convolution and the “goodness of fit” decided on the basis of χ^2 values and the distribution of residuals.

3. Results and discussion

The aim of this work was to study the properties of aza-crown ether substituted derivatives of 3-hydroxyflavone and assess their suitability as fluorescent sensors for metal ions. As the mechanism of the sensing action would involve interference with the charge transfer interaction of the nitrogen of the aza crown ether with the 3-hydroxyflavone system, it was first decided to study the protonation properties of the compounds. Protonation of the nitrogen atom should completely remove the possibility of lone pair donation into the hydroxyflavone system; similar to the effects that might be anticipated if the aza crown ether ring were complexed to a metal cation.

4. Protonation properties of **1a**, **1b**, **3a** and **3b**

The effect of acidity on the absorption and emission properties of **1a**, **1b**, **3a** and **3b** was studied in aqueous ethanolic solutions (50/50, v/v) by varying the amount of added hydrochloric acid. For **1a** and **1b**, the ionic strength was maintained at a constant 1.0 mol dm^{-3} with sodium chloride solution, but for **3a** and **3b**, which can complex with sodium ions, the ionic strength varied with the concentration of hydrochloric acid. In all four cases the behaviour of the absorption spectra of the aqueous ethanolic solutions was the same; the most intense UV-Vis absorption band in the region of 400 nm decreased in intensity with increasing acid concentration and was replaced by a pair of new absorption bands in the 300–360 nm region. The spectral changes occurred largely over a range of acid concentration between 1 mmol dm^{-3} and 1 mol dm^{-3} and the final absorption spectra were very

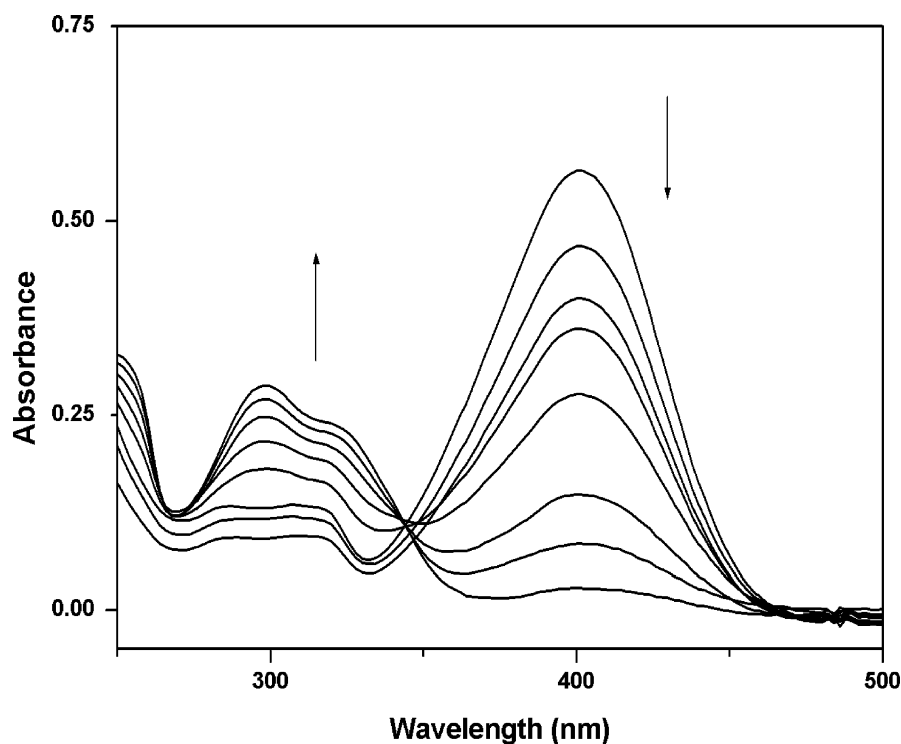


Fig. 1. Absorption spectra of **1b** (concentration $1.40 \times 10^{-5} \text{ mol dm}^{-3}$) in 50/50 (v/v) ethanol/water at $[\text{H}^+]$ of 0, 0.005, 0.01, 0.05, 0.1 and 0.25 mol dm^{-3} . The arrows indicate the changes of peak intensity with increasing acidity.

similar to those of 3-hydroxyflavone (for **1a** and **3a**) or 3-methoxyflavone (for **1b** and **3b**). A typical set of absorption spectra are shown in Fig. 1 for compound **1b**. $\text{p}K_{\text{b}}$ values were calculated for all four compounds from the spectra and are given in Table 1. For both pairs of compounds, the ground state of the hydroxy derivative is more easily protonated than the methoxy. In addition, the two dimethylamino compounds are more easily protonated than the two aza crowns. The latter presumably reflects the different steric interactions between the amino substituents and the 3'- and 5'-hydrogens on the phenyl ring whereas the former observation is associated with the ability of **1a** and **3a** to undertake a wider range of inter- and intra-molecular hydrogen bonding interactions.

Fluorescence spectra (excited at the isosbestic point in the absorption spectra) were measured over the same range of acid concentration. The emission spectra of **1a** and **3a** in aqueous ethanol comprise single bands peaking at approximately 530 nm and 520 nm respectively. The emission intensity of both compounds decreased steadily as the $[\text{H}^+]$ was increased and shifted slightly to the red, but there was

no compensating increase in emission elsewhere in the spectrum. This reflects the fact that when the possibility of TICT state formation is removed by protonating the dialkylamino group, **1a** and **3a** still undergo ESIPT and, by coincidence, the emission spectra of the TICT and ESIPT states are spectrally similar. The fluorescence quantum yield of the latter is smaller [8], however, thus accounting of the decrease in intensity. Analysis of the emission spectral intensities as a function of $[\text{H}^+]$ yielded $\text{p}K_{\text{b}}^*$ values of 2.11 and 1.50 (Table 1). These are essentially identical to the ground state values indicating that the distribution of excited state species is determined by the absorption spectrum. This finding is in accord with the rapidity with which the "normal" LE state undergoes ESIPT [6] or is converted to the TICT state [8] and the short lifetimes of the latter.

1b, however, exhibits the expected emission behaviour in that as the $[\text{H}^+]$ is increased, TICT state emission in the 450–650 nm wavelength range is replaced by LE emission peaking at approximately 400 nm (Fig. 2); ESIPT is impossible in **1b**. Once again the $\text{p}K_{\text{b}}^*$ value of 1.71 is found to be very similar to the ground state $\text{p}K_{\text{b}}$. Fig. 2 shows very clearly the excellent separation between the two emitting species exhibit similar emission intensities, allowing accurate ratioing of the relative intensities. **1b** should therefore be a viable ratiometric fluorescent proton sensor for concentrations between 0.1 and $0.001 \text{ mol dm}^{-3}$. Compound **3b** behaves in a similar manner to **1b** for the most part but there is a greater discrepancy between the

Table 1
 $\text{p}K_{\text{b}}$ values for compounds **1a**, **1b**, **3a** and **3b**

Compound	$\text{p}K_{\text{b}}$	$\text{p}K_{\text{b}}^*$
1a	2.20	2.11
1b	1.78	1.71
3a	1.35	1.50
3b	0.79	1.26

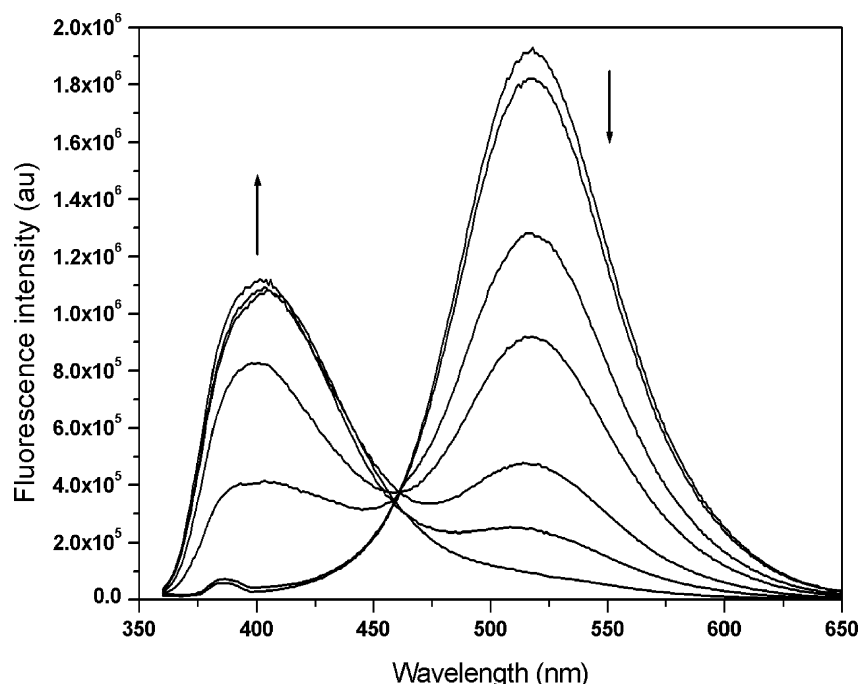


Fig. 2. Fluorescence spectra of **1b** (concentration $1.40 \times 10^{-5} \text{ mol dm}^{-3}$) in 50/50 (v/v) ethanol/water at $[\text{H}^+]$ of 0, 0.005, 0.01, 0.05, 0.1 and 0.25 mol dm^{-3} . The arrows indicate the changes of peak intensity with increasing acidity.

ground and excited state $\text{p}K_{\text{b}}$ values suggesting that there is a further interaction between **3b** and protons in the excited state.

Fluorescence lifetimes were measured for **1a** and **1b** as a function of acid concentration under the same conditions as the emission spectra described above. Unfortunately, the lifetimes of both compounds in mixed aqueous/organic solvents are much shorter than in pure organic solvents [8] and, in the case of **1b** are at (or below) the resolution of the equipment. For this compound, at all emission wavelengths and acidities studied, the fluorescence decays are dominated by a short-lived component of 150–200 ps. In the case of **1a** however, in 1.0 mol dm^{-3} sodium chloride, a single exponential decay with a lifetime of 600 ps is observed. As the acidity of the medium is increased, the decays become biexponential—the two components having lifetimes of 200 and 600 ps (using global analysis of the data)—with the shorter lived component becoming more important with increasing $[\text{H}^+]$. The relative proportions of the two components correlate quite well with the concentrations of the neutral and protonated forms of **1a**.

5. Complexation of **3a**, **3b** and **4a** with alkali metal and alkaline earth cations

The complexation of the two 15-crown-5 compounds **3a** and **3b** with alkali metal and alkaline earth cations was studied in acetonitrile. The metal perchlorates are soluble in this solvent up to high mM concentrations and the absence of any significant amounts of water means that the excited

singlet states are not quenched as they are in aqueous or aqueous/organic solvents. Both compounds exhibit a single absorption peak above 250 nm in acetonitrile; with λ_{max} values of 400 nm and 382 nm for **3a** and **3b** respectively and a $\log \epsilon$ of 4.49 for both compounds. **3a** exhibits dual emission bands in acetonitrile with peaks at approximately 510 and 565 nm, whereas **3b** exhibits a single band at 480 nm. The fluorescence decay profile for the latter is a clean single exponential of lifetime 2.50 ns whereas **3a** is biexponential with the majority (97%) of the decay in a relatively short-lived component of approximately 400 ps and the remainder in a longer-lived component of $\sim 3.5 \text{ ns}$.

Addition of alkali metal or alkaline earth perchlorates to the acetonitrile solutions of **3a** and **3b** led to three kinds of behaviour as far as the absorption spectra are concerned. K^+ and Cs^+ appeared to have no effect on the absorption spectrum of **3a** up to concentrations of 50 mM. Higher concentrations of the two ions were achieved in 50/50 (v/v) acetonitrile/water mixtures but, once again, no significant changes in the absorption spectra were observed. The second kind of behaviour is typified by the spectral changes for **3a** in the presence of barium (Fig. 3) and is the most commonly observed behaviour (**3a** with Li^+ , Na^+ , Ca^{2+} and Ba^{2+} and **3b** with all the metal ions used in this study). The main absorption band decreases in intensity as the metal ion concentration increases and is replaced by new absorption features at shorter wavelength. This behaviour for **3a** and with Ba^{2+} has been previously reported by Roshal et al. [11]. These spectral variations allowed the calculation of binding constants [31] for the various ionophore/metal ion combinations which are reported in Table 2.

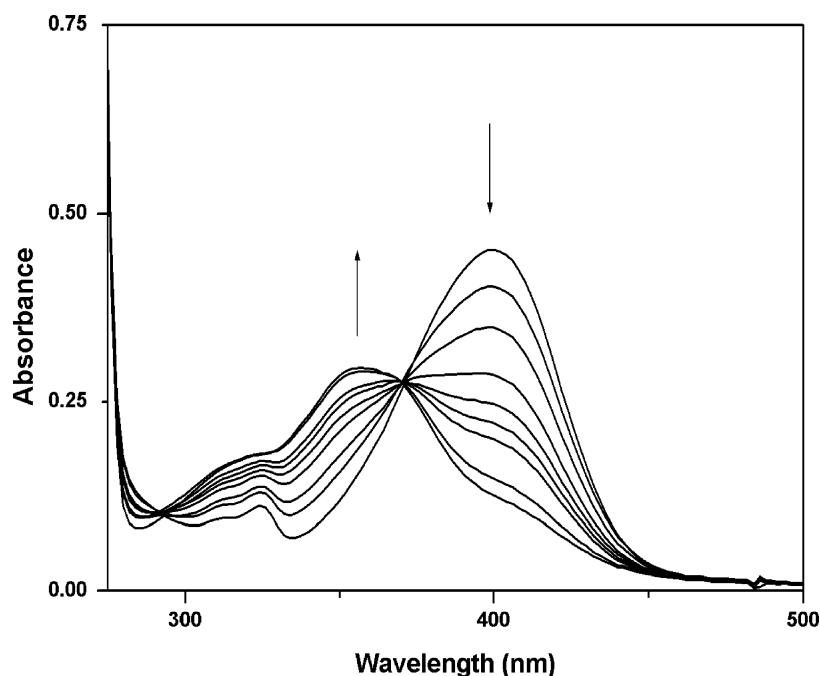
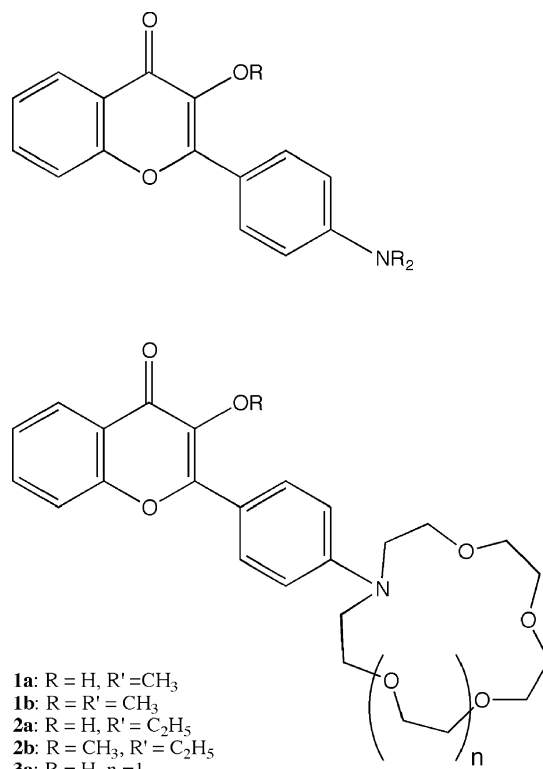


Fig. 3. Absorption spectra of **3a** (concentration $1.50 \times 10^{-5} \text{ mol dm}^{-3}$) in acetonitrile in the presence of Ba^{2+} , concentration range 0.0–3.0 mmol dm^{-3} . The arrows indicate the changes of peak intensity with increasing $[\text{Ba}^{2+}]$.

The final kind of behaviour was unique to compound **3a** with Mg^{2+} . Here the initial change in the absorption spectra was the appearance of a shoulder ($\lambda_{\text{max}} \approx 470 \text{ nm}$) on the red edge of the main absorption band concurrent with a decrease in intensity of the latter (Fig. 4). These changes are quite “clean” up to a Mg^{2+} concentration of the order of 1 mM. At higher Mg^{2+} concentrations a third absorption feature, intermediate (in wavelength terms) between the other two, appears. Again, this behaviour has been reported by Roshal et al. [11], and binding constants have been calculated.

These spectral changes have been attributed [11] to **3a** binding 2 moles of Mg^{2+} . The first ion binds to the carbonyl group and a deprotonated 3-hydroxyl group and the second ion binds to the aza crown ring (Schemes 1 and 2). The need for the 3-hydroxyl group to deprotonate to allow the Mg^{2+} to bind explains why similar behaviour is not observed for **3b**. In all the other combinations that we have studied, the



Scheme 1. Structures of cited compounds.

Table 2

Binding constants (K_s) for **3a**, **3b** and **4a** with alkali metal and alkaline earth cations in acetonitrile

Metal ion	3a log K_s	3b log K_s	4a log K_s
Li^+	2.6	2.4	–
Na^+	1.8	2.0	–
K^+	<0.5	2.1	–
Cs^+	<0.5	2.2	–
Mg^{2+}	4.4 (2.25 ^a), 2.9 (0.83 ^a)	2.4	3.8, 1.9
Ca^{2+}	4.0	3.7	5.0, 1.1
Ba^{2+}	3.4 (2.4 ^a), (0.89 ^a)	3.0	4.9, 0.9

^a Literature values from ref. [11].

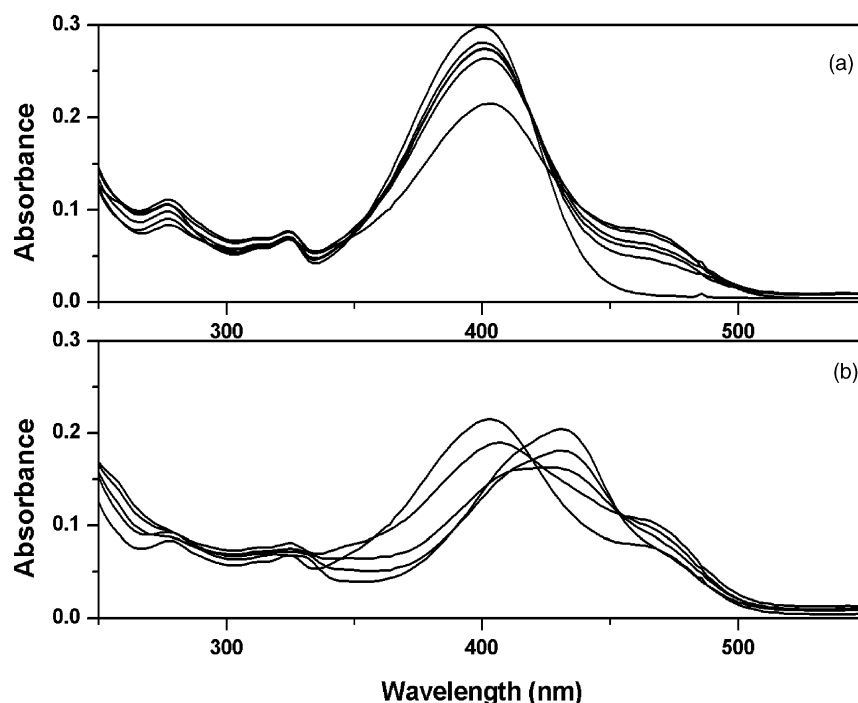
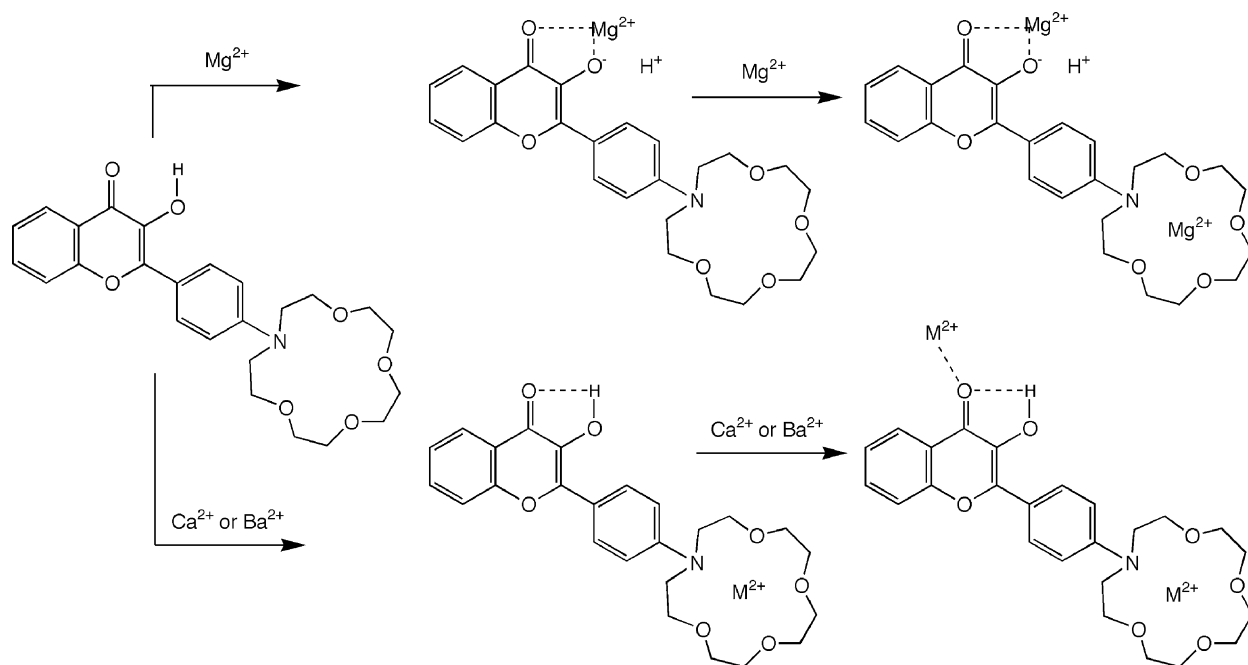


Fig. 4. Absorption spectra of **3a** (concentration $1.00 \times 10^{-5} \text{ mol dm}^{-3}$) in acetonitrile in the presence of Mg^{2+} , concentration ranges; (a) 0.0–1.0 mmol dm^{-3} ; (b) 1.0–10.0 mmol dm^{-3} .

metal ion binds to the aza crown ether moiety first. Roshal et al. [11] report that Ba^{2+} also forms a double complex with **3a** but in the reverse order to Mg^{2+} , ie the first Ba^{2+} ion binds to the aza crown and the second to the carbonyl and deprotonated 3-hydroxyl group. We did not observe this

behaviour for **3a** with either Ba^{2+} or Ca^{2+} but this may be a consequence of our not using sufficiently high metal ion concentrations. We are concerned at the discrepancy between the binding constants calculated here and those reported by Roshal et al. [11] (Table 2) although we note that the two



Scheme 2. The species produced on binding alkaline earth cations to **3a** (and **4a**).

values for **3a** with Mg^{2+} that we report vary by the same two orders of magnitude from the corresponding literature values. We are unable to account for these differences.

Somewhat surprisingly, the emission properties of **3a** and **3b** in acetonitrile in the presence of the Groups I and II metal ions bear little resemblance to the behaviour observed in the presence of H^+ described above. In the case of **3b** the emission of the uncomplexed compound ($\lambda_{\text{max}} \approx 480 \text{ nm}$) undergoes a slight blue shift (up to 10 nm) and decreases in intensity by up to an order of magnitude depending on the metal ion present and its concentration. This may be compared with the much larger band shift and retained emission intensity in the presence of H^+ (Fig. 2). The biggest effects are caused by the dipositive alkaline earth ions in the order $[\text{Ca}^{2+}] > [\text{Mg}^{2+}] > [\text{Ba}^{2+}] \gg [\text{M}^+]$. This does not quite follow the same order as the binding constants, but it is clear that the size of the binding constant is only one of the factors which affect the emission intensity since Li^+ , which has the same measured binding constant with **3b** as Mg^{2+} , has only about 1% of the effect of the same concentration of Mg^{2+} on the **3b** emission.

At low concentrations ($< 100 \mu\text{M}$) of M^{2+} , the reduction of the emission intensity of **3b** yields a linear Stern–Volmer plot with apparent quenching rate constants of 3.8×10^{11} , 1.1×10^{11} and $6.6 \times 10^{10} \text{ dm}^3 \text{ mol}^{-1} \text{ s}^{-1}$ for Ba^{2+} , Mg^{2+} and Ca^{2+} , respectively. At higher concentrations the linearity is lost and the emission intensity tends towards a plateau value. These apparent Stern–Volmer rate constants are much larger than would be expected on the basis of diffusion control and suggest that other processes are also operating. Indeed, on the basis of the K_s values in Table 2, the observed quenching can largely be ascribed to static quenching as a result of the ground state complexation that occurs in the 0–100 μM concentration range. This is backed up by measurements of the fluorescence lifetime of **3b** as a function of metal ion concentration (specifically Mg^{2+}) which produce a picture rather different to that provided by the emission spectra. The lifetime of uncomplexed **3b** in acetonitrile is 2.50 ns (clean, single exponential fit). As Mg^{2+} ions are added to the solution, the fluorescence decay continues to be adequately fitted by a single exponential but the lifetime decreases. However, the observed decrease in fluorescence lifetime is only a fraction of the observed decrease in fluorescence emission intensity. For example, in the presence of 20 mM Mg^{2+} , the emission intensity of **3b** is about one-fifth of the intensity of the uncomplexed compound, whereas the fluorescence lifetime has only decreased to 2.14 ns (a reduction of 14% compared to 80% in the emission intensity). The variation of lifetime with $[\text{Mg}^{2+}]$ also appears to follow a Stern–Volmer relationship over the concentration range studied (0–20 mM) with a quenching rate constant of $3.3 \times 10^9 \text{ dm}^3 \text{ mol}^{-1} \text{ s}^{-1}$. This value is much more in line with that expected for a diffusional quenching process.

The fluorescence spectra of **3a** only exhibit significant changes in the presence of the alkaline earth cations, however these changes are quite drastic. The spectra of the free

3a in acetonitrile exhibit peaks at approximately 500 nm and 565 nm. At low concentrations (0–3.0 mM) of Ca^{2+} or Ba^{2+} , these two bands merge into one (Fig. 5) and then, at higher concentrations (10–100 mM), greatly increase in intensity and slightly blue-shift. Roshal et al. [11] report identical behaviour for **3a** with Ba^{2+} . Despite the different mechanism which is operating when **3a** complexes with Mg^{2+} , the emission spectra at first sight appear to change in a similar manner to that described above for Ca^{2+} and Ba^{2+} . The formation of the initial complex ($[\text{Mg}^{2+}] = 0\text{--}20 \mu\text{M}$) is accompanied by a swift merger of the two emission bands of free **3a** into a single band peaking around 520 nm, although the longer wavelength of the two initial bands is clearly present as a shoulder (Fig. 6). At higher concentrations (100 μM –10 mM), increased emission intensity is accompanied by the appearance of a new emission band around 470 nm which combines with the 520 nm band to cause the overall emission maximum to shift to shorter wavelengths. Again, these observations parallel those reported by Roshal et al. [11].

The fluorescence decay profile of **3a** in acetonitrile is virtually identical to that of **2a** in the same solvent—a biexponential decay with lifetimes of 380 ps and 3.0–4.0 ns which is dominated by the former (>95% of the decay) at all emission wavelengths. As a consequence the longer lived component is somewhat poorly defined in terms of its lifetime. Addition of Mg^{2+} does not appear to affect the biexponentiality of the decay or the lifetime values, but the relative intensity shifts in favour of the longer-lived component, eg from 70%/30% at 0.5 mM Mg^{2+} to approximately 50%/50% at 2.5 mM to 15%/85% at 10 mM.

The behaviour of **4a** in the presence of the alkaline earth cations is virtually identical to that of **3a** as far as the absorption and emission properties are concerned. However, the binding constants for the three metal ions are different to those for **3a** (Table 2) and here we also observe the binding of a second cation at higher concentrations of Ca^{2+} and Ba^{2+} ; as observed by Roshal et al. [11] for **3a** with Ba^{2+} (but not observed by us for this combination). Fluorescence lifetime data for **4a** was recorded over a wide range of $[\text{M}^{2+}]$ and at discrete wavelengths across the emission spectrum. The observed behaviour is similar to that for **3a** at lower metal ion concentrations in that there is a shift in intensity from a short-lived lifetime component (400–500 ps) to a longer-lived one (3.65 ns). However, at higher concentrations of the metal ions, the decay profiles are wavelength dependent and exhibit a rise component in some of the decays. This data will be reported in depth at a later date.

The compounds reported here have similar binding constants for the alkali metal and alkaline earth cations to those reported by Valeur and co-workers for a monoaza-15-crown-5 attached to a benzoxazinone (BOZ-crown) or a dicyanomethylenepyrans (DCM-crown) [32]. The three alkaline earth dications bind to a monoaza-15-crown-5 with stability constants of the order of $10^4 \text{ dm}^3 \text{ mol}^{-1}$ and the alkali metals Li^+ and K^+ with stability constants approximately

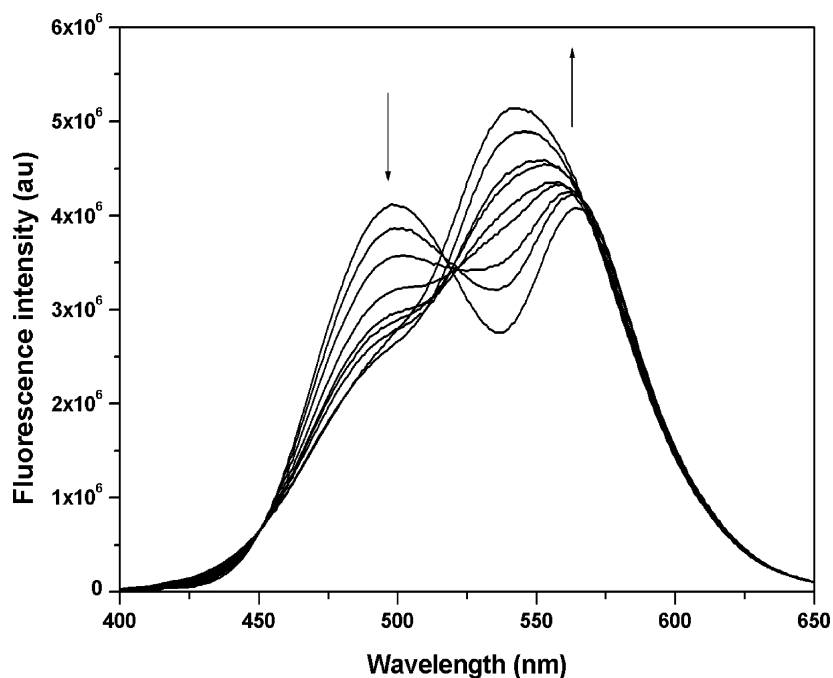


Fig. 5. Fluorescence spectra of **3a** (concentration $1.50 \times 10^{-5} \text{ mol dm}^{-3}$) in acetonitrile in the presence of Ba^{2+} , concentration range $0.0\text{--}3.0 \text{ mmol dm}^{-3}$. The arrows indicate the changes of peak intensity with increasing $[\text{Ba}^{2+}]$.

two orders of magnitude lower. These stability constants appear to be roughly independent of the attached chromophore and fluorophore—as long as the latter does not contribute to the binding of the metal ion. In cases where the chromo/fluorophore also binds to the metal ion (e.g. in a number of coumarin-linked 15-crown-5 molecules [33]) the stability constants are increased.

The two hydroxyflavone-crowns **3a** and **4a** offer an interesting variation on the properties which are usually observed for crown-linked compounds in that the complexation of two metal ions per crown compound extends the concentration range over which complexation occurs. In addition, the observed spectral changes allow clear differentiation between the binding of the first metal ion (when the

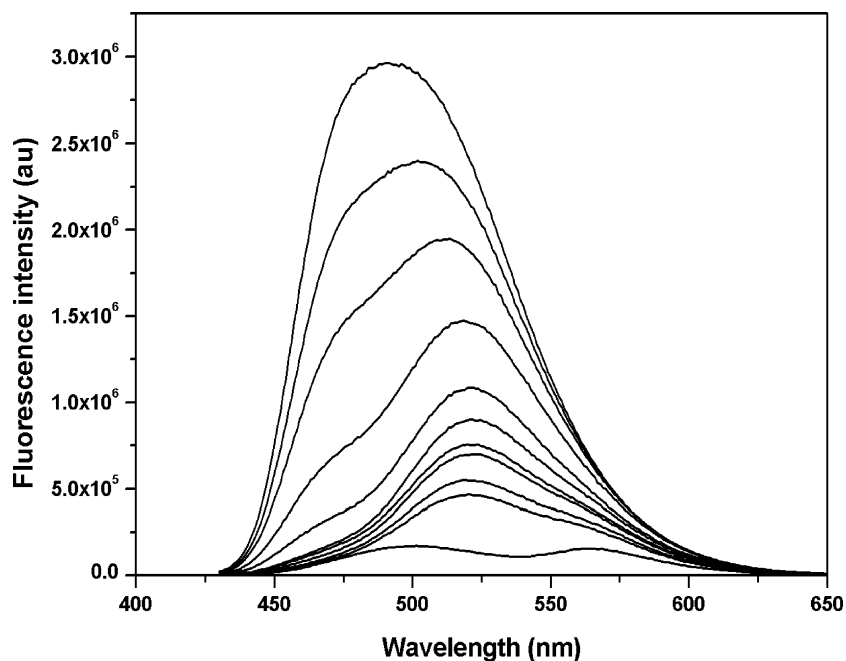


Fig. 6. Fluorescence spectra of **3a** (concentration $1.00 \times 10^{-5} \text{ mol dm}^{-3}$) in acetonitrile in the presence of Mg^{2+} , concentration range $0.0\text{--}10.0 \text{ mmol dm}^{-3}$.

two emission peaks merge) and the second metal ion (when large intensity increases are observed). Unfortunately, the monoaza-15-crown-5 and 18-crown-6 rings are both insufficiently selective in terms of the metal ions that they sense.

Acknowledgements

We thank BNFL plc (studentship for XP) and the University of Central Lancashire for financial assistance and the European Union for providing access to HASYLAB (project II-97-02 EC).

References

- [1] A.W. Czarnik, in: A.W. Czarnik (Ed.), *Fluorescent Chemosensors for Ion and Molecule Recognition*, ACS Books, Washington, DC, 1993; A.W. Czarnik, *Acc. Chem. Res.* 27 (1994) 302; J.R. Lakowicz (Ed.), *Topics in Fluorescence Spectroscopy*, vol. 4, *Probe Design and Chemical Sensing*, Plenum Press, New York, 1994.
- [2] A.P. de Silva, H.Q.N. Gunaratne, T. Gunnlagsson, A.J.M. Huxley, C.P. McCoy, J.T. Rademacher, T.E. Rice, *Chem. Rev.* 97 (1997) 1515.
- [3] J.-F. Létard, S. Delmond, R. Lapouyade, D. Braun, W. Rettig, M. Kreissler, *Rec. Trav. Chim. Pays-Bas* 114 (1995) 517.
- [4] W. Rettig, R. Lapouyade, in: J.R. Lakowicz (Ed.), *Topics in Fluorescence Spectroscopy, Probe Design and Chemical Sensing*, vol. 4, Plenum Press, New York, 1994, p. 109.
- [5] W. Rettig, *Angew. Chem. Int. Ed. Engl.* 25 (1986) 971.
- [6] S.M. Ormson, R.G. Brown, *Progr. React. Kinet.* 19 (1994) 45; D. Le Gourrieréc, S.M. Ormson, R.G. Brown, *Progr. React. Kinet.* 19 (1994) 211.
- [7] J. Kawakami, Y. Komai, T. Sumori, A. Fukushi, K. Shimozaki, S. Ito, *J. Photochem. Photobiol. A* 139 (2001) 71.
- [8] S.M. Ormson, R.G. Brown, F. Vollmer, W. Rettig, *J. Photochem. Photobiol. A: Chem.* 81 (1994) 65.
- [9] X. Poteau, R.G. Brown, in: *Proceedings of the XVIth IUPAC Photochemistry Symposium*, Helsinki, 1996.
- [10] V.G. Pivovarenko, A.D. Roshal, A.P. Demchenko, in: *Proceedings of the XVIth IUPAC Photochemistry Symposium*, Helsinki, 1996.
- [11] D. Roshal, A.V. Grigorovich, A.O. Doroshenko, V.G. Pivovarenko, A.P. Demchenko, *J. Phys. Chem. A* 102 (1998) 5907.
- [12] P. Wang, S. Wu, *Chem. Res. Chin. Univ.* 14 (1998) 379.
- [13] W. Liu, J. Tang, Y. Wang, G. Shen, R. Yu, *Fresenius J. Anal. Chem.* 362 (1998) 387.
- [14] W. Liu, Y. Wang, J. Tang, G. Shen, R. Yu, *Anal. Sci.* 14 (1998) 547.
- [15] W. Liu, Y. Wang, W. Jim, G. Shen, R. Yu, *Anal. Chim. Acta* 383 (1999) 299.
- [16] Sytink, D. Gormin, M. Kasha, *Proc. Natl. Acad. Sci. U.S.A.* 91 (1994) 11968.
- [17] V.G. Pivovarenko, A.V. Tuganova, A.S. Klimchenko, A.P. Demchenko, *Cell. Molec. Biol. Lett.* 2 (1997) 355.
- [18] M. Dennison, J. Guharay, P.K. Sengupta, *Spectrochim. Acta Part A* 55A (1999) 903; M. Dennison, J. Guharay, P.K. Sengupta, *Spectrochim. Acta Part A* 55A (1999) 1127; M. Dennison, J. Guharay, P.K. Sengupta, *J. Surf. Sci. Technol.* 16 (2000) 105.
- [19] P.-T. Chou, M.L. Martinez, J.H. Clements, *Chem. Phys. Lett.* 204 (1993) 395.
- [20] Klymchenko, T. Ozturk, V.G. Pivovarenko, A.P. Demchenko, *Tet. Lett.* 42 (2001) 7967.
- [21] C. Swinney, D.F. Kelley, *J. Chem. Phys.* 99 (1993) 211.
- [22] P.-T. Chou, M.L. Martinez, J.H. Clements, *J. Phys. Chem.* 97 (1993) 2618.
- [23] P. Wang, S. Wu, *J. Photochem. Photobiol. A* 76 (1993) 27.
- [24] P. Wang, S. Wu, *J. Lumin.* 62 (1994) 33.
- [25] N.A. Memkovikh, J.V. Kruchenok, A.N. Rubinov, V.G. and W. Baumann, *J. Photochem. Photobiol. A* 139 (2001) 53; J.V. Kruchenok, N.A. Nemkovitch, A.N. Sobchuk, E.P. Petrov, A.N. Rubinov, V.G. Pivovarenko, W. Baumann, *Proc. SPIE* 4749 (2002) 413.
- [26] J.P. Dix, F. Vögtle, *Chem. Ber.* 113 (1980) 457.
- [27] R.A. Schultz, B.D. White, D.M. Dishong, K. Arnold, G.W. Gokel, *J. Am. Chem. Soc.* 107 (1985) 6659.
- [28] D.V. O'Connor, D. Phillips, *Time-Correlated Single Photon Counting*, Academic Press, New York, 1984.
- [29] R. Sparrow, R.G. Brown, E.H. Evans, D. Shaw, *J. Chem. Soc., Faraday Trans. 2* 82 (1986) 2249.
- [30] C. Spies, R. Gehrke, *Macromolecules* 30 (1997) 1701.
- [31] J.-L. Habib Jiwan, C. Branger, J.-Ph. Soumillion, B. Valeur, *J. Photochem. Photobiol. A* 116 (1998) 127.
- [32] S. Fery-Forgues, J. Bourson, L. Dallery, B. Valeur, *New J. Chem.* 14 (1990) 617.
- [33] B. Valeur, F. Badaoui, E. Bardez, J. Bourson, P. Boutin, A. Chatelin, I. Devol, B. Larrey, J.P. Lefèvre, A. Soulet, in: J.P. Desvergne, A. W. Czarnik (Eds.), *Chemosensors of Ion and Molecule Recognition*, Kluwer Academic Publishers, Netherlands, 1997, p. 195.